HAL open science

Made-to-order metal-organic frameworks for trace carbon dioxide removal and air capture

Osama Shekhah, Youssef Belmabkhout, Zhijie Chen, Vincent Guillerm, Amy Cairns, Karim Adil, Mohamed Eddaoudi

To cite this version:

Osama Shekhah, Youssef Belmabkhout, Zhijie Chen, Vincent Guillerm, Amy Cairns, et al.. Made-to-order metal-organic frameworks for trace carbon dioxide removal and air capture. Nature Communications, 2014, 5, pp.4228. 10.1038/ncomms5228 . hal-02360096

HAL Id: hal-02360096

https://hal.science/hal-02360096

Submitted on 12 Nov 2019

HAL is a multi-disciplinary open access archive for the deposit and dissemination of scientific research documents, whether they are published or not. The documents may come from teaching and research institutions in France or abroad, or from public or private research centers.

L'archive ouverte pluridisciplinaire **HAL**, est destinée au dépôt et à la diffusion de documents scientifiques de niveau recherche, publiés ou non, émanant des établissements d'enseignement et de recherche français ou étrangers, des laboratoires publics ou privés.

nature
COMMUNICATIONS

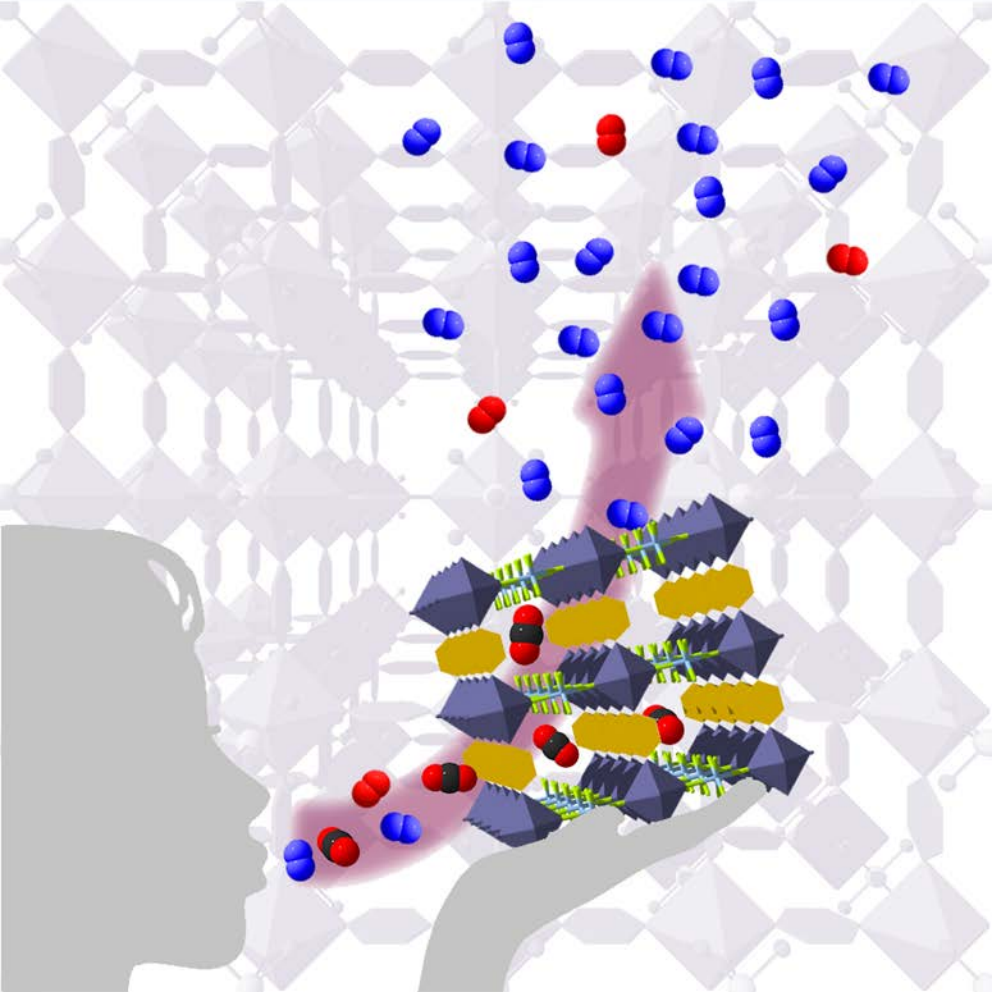

nature COMMUNICATIONS

ARTICLE

Received 9 Nov 2013 | Accepted 28 May 2014 | Published 25 Jun 2014

DOI: 10.1038/ncomms5228

OPEN

Made-to-order metal-organic frameworks for trace carbon dioxide removal and air capture

Osama Shekhah[1,*], Youssef Belmabkhout[1,*], Zhijie Chen[1], Vincent Guillerm[1], Amy Cairns[1], Karim Adil[1] & Mohamed Eddaoudi[1]

Direct air capture is regarded as a plausible alternate approach that, if economically practical, can mitigate the increasing carbon dioxide emissions associated with two of the main carbon polluting sources, namely stationary power plants and transportation. Here we show that metal-organic framework crystal chemistry permits the construction of an isostructural metal-organic framework (**SIFSIX**-3-Cu) based on pyrazine/copper(II) two-dimensional periodic 4^4 square grids pillared by silicon hexafluoride anions and thus allows further contraction of the pore system to 3.5 versus 3.84 Å for the parent zinc(II) derivative. This enhances the adsorption energetics and subsequently displays carbon dioxide uptake and selectivity at very low partial pressures relevant to air capture and trace carbon dioxide removal. The resultant **SIFSIX-**3-Cu exhibits uniformly distributed adsorption energetics and offers enhanced carbon dioxide physical adsorption properties, uptake and selectivity in highly diluted gas streams, a performance, to the best of our knowledge, unachievable with other classes of porous materials.

[1] Functional Materials Design, Discovery and development (FMD[3]), Advanced Membranes and Porous Materials (AMPM); Physical Sciences and Engineering Division, King Abdullah University of Science and Technology (KAUST), Thuwal 23955-6900, Kingdom of Saudi Arabia. * These authors contributed equally to this work. Correspondence and requests for materials should be addressed to M.E. (email: mohamed.eddaoudi@kaust.edu.sa).

© 2014 Macmillan Publishers Limited. All rights reserved.

The amount of carbon dioxide (CO_2) in the atmosphere continues to rise and rather rapidly due to unparalleled cumulative CO_2 emissions, provoking the undesirable greenhouse gas effect. Certainly, it is becoming critical to develop economical and practical pathways to reduce the CO_2 emissions; and appropriately prospective routes to address this enduring challenge are considered: (i) CO_2 emission reduction from post-combustion stationary and mobile sources[1] where CO_2 concentration is in the range of 10–15% and (ii) CO_2 removal from air called direct air capture (DAC), which is another alternative option to reduce greenhouse gases emissions in a uniform way globally[1–4]. Although DAC is relatively more challenging than post-combustion capture, it is recognized that it might be practical, provided that suitable adsorbent combining optimum uptake, kinetics, energetics and CO_2 selectivity is available at trace CO_2 concentration[5].

In addition, efficient and cost-effective removal of trace CO_2 is of prime importance in various key industrial applications pertaining to energy, environment and health. From an industrial perspective, the removal of trace CO_2 from air is a growing area of research and development due to its substantial importance for prepurification of air and particularly when atmospheric air is used during the separation of nitrogen and oxygen. In fact, before air separation using cryogenic distillation or pressure swing adsorption, air must be CO_2 free to avoid (i) blockage of heat-exchange equipment as a result of frozen CO_2 during the liquefaction process[6,7] and (ii) adsorbents (for example, zeolites) contamination used for oxygen production by pressure swing adsorption[8–10].

Equally important, alkaline fuel cells require a CO_2 free feedstock of oxygen and hydrogen gases as it is widely recognized that trace amounts of CO_2 (that is, 300 p.p.m.) degrade the electrolyte in alkaline fuel cells[11]. Furthermore, efficient removal of CO_2 at low concentrations is also vital for the proper operation of breathing systems in confined spaces such as submarines and aerospace shuttles[12–14]. In fact, in long-term space flight and submarine missions, CO_2 must be removed from the air and recycled because resupply opportunities are scarce. An average crew member requires approximately 0.84 kg of oxygen and emits approximately 1 kg of CO_2 per day[14]. Thus, the ability to continuously purify the exhaled air (with a maximum CO_2 concentration of 2–5%) will lead to an optimal recycling and considerable reduction in fresh air supply in remote confined spaces.

Efficient CO_2 removal and resupply of fresh air is also critical in mining and rescue missions[15], diving and most importantly in medical applications such as anaesthesia machines[16]. The use of anaesthesia machines is still a growing clinical trend worldwide, driven by the need to reduce cost and improve patient care via the use of efficient CO_2 sorbents. The CO_2 removal feature in anaesthesia machines is particularly important in semi-closed or closed rebreathing systems, as the rebreathing fraction is at least 50% of the exhaled gas volume, directed back to the patient after proper CO_2 removal in the next exhalation. Sodalime is currently the sorbent of choice in most commercially available anaesthesia machines. This sorbent exhibits a high CO_2 removal efficiency from exhaled air, with an average continuous operation of about 24 h using a prepacked commercial cartridge[17]. Nevertheless, a major drawback of this technology is that one sodalime cartridge can only be used for a single cycle and is non-recyclable, therefore generating undesirable waste as it should be disposed properly.

Evidently, there is a pressing need to develop novel porous materials[18] that can adequately address the growing interest in low CO_2 concentration removal applications[10]. It is important to mention that only few materials were reported to efficiently adsorb traces of CO_2, particularly with regards to DAC using a variety of amine-supported materials (for example, porous silica)[10,19].

Our quest for made-to-order materials that can address efficiently the separation and capture of trace CO_2 has prompted us to explore the potential of a burgeoning class of modular and tunable porous materials, namely metal-organic frameworks (MOFs), to tackle this ongoing challenge. Recently, MOFs were investigated intensively for intermediate and high CO_2 concentration removal applications such as post-combustion and precombustion capture, natural gas and biogas upgrading[20–23]. Nevertheless, the potential of MOFs to remove trace and low CO_2 concentration from gas streams was rarely debated[24–28]. The main reason for this lack of studies is that most of MOFs reported so far, with or without unsaturated metal centres or/and functionalized ligands, exhibit relatively low CO_2 uptake and selectivity particularly at relatively low CO_2 partial pressure. To overcome this downfall, various research groups have adopted the amine grafting chemistry and the acquired knowledge from amine-supported silica[19,22] as a prospective pathway to enhance the CO_2 adsorption energetics and uptake in MOFs and covalent organic frameworks[27–29]. Particularly, Jones and co-workers[28] reported for the first time the effect of ethylenediamine grafting on Mg-MOF-74 as a support for CO_2 adsorption from ultradilute gas streams such as ambient air. Correspondingly, Long and co-workers investigated the effect of *N,N*-dimethylethylenediamine grafting for DAC using an expanded isostructure of Mg-MOF-74 (ref. 27). Markedly, the few reported strategies targeting air capture using MOFs are centred on the aptitude of grafted amines to form a strong chemical bond (at least 70 kJ mol^{-1}) with CO_2, affording high affinity toward CO_2 and therefore high CO_2 selectivity.

There is no reported study hitherto, to the best of our knowledge, on tuning the pore size of physical adsorption–based MOFs to target trace and low-concentration CO_2 removal. In this communication, we report how the reasoned choice of the appropriate MOF platform (here, **SIFSIX**-3-Cu material), characterized by suitable pore size, combined with the optimal CO_2 energetics (that is, strong, uniform and relatively low to allow reversible physical adsorption–desorption), is the key to target made-to-order porous materials for trace and low CO_2 concentration removal in general and DAC application in particular.

Results

Preparation and characterization of SIFSIX-3-Cu analogue. The **SIFSIX**-3-Cu analogue was successfully prepared by layering a methanol solution of pyrazine in a glass tube onto a methanol solution of $CuSiF_6 \times H_2O$. On layering, an extremely fast formation of light violet powder was observed, which was left for 24 h in the mother solution. The powder was then collected and washed extensively with methanol then dried under vacuum and characterized using powder X-ray diffraction (PXRD).

The PXRD diagram of **SIFSIX**-3-Cu analogue studied in this work was found not to match any related reported structures, that is, the Cu-2D structures or the 3D Zn analogue reported by Kita and co-workers[30] (Supplementary Fig. 1). Despite extensive attempts, we were not able to isolate synthetic conditions affording single crystals of sufficient size suitable for single crystal diffraction studies and therefore structural determination by powder diffractometry was explored.

The PXRD pattern of the crystalline powder, resulting from the reaction of $CuSiF_6 \times H_2O$ with pyrazine in methanolic solution, was recorded on a high resolution PANalytical X'Pert MPD-PRO diffractometer with Cu–Kα radiation ($\lambda = 1.5406$ Å) in the range

© 2014 Macmillan Publishers Limited. All rights reserved.

of 4 to 80° using a step of 0.05° (250 s per step). The indexation of the PXRD diagram, carried out using the McMaille software[30], yielded a primitive orthorhombic cell ($M(20)=42.3$ and $F(20)=39.9$ (0.0139, 36)). The cell parameters, $a=b=6.919(1)$ Å, $c=7.906(1)$ Å, were refined by a whole powder pattern fit using the Le Bail method[31], implemented in the FULLPROF software[32], and were consistent with those of the previously described **SIFSIX**-3-Zn. Hence, atomic positions of the latter were used as structure solution. The final Rietveld refinement permitted access to satisfactory results: $R_{Bragg}=0.051$ and $R_{Factor}=0.056$ (Supplementary Fig. 2). The crystallographic data and refinement parameters of **SIFSIX**-3-Cu are summarized in Supplementary Table 1.

As initially expected, it is in very good agreement with the 3D structure of the Zn analogue reported previously (Fig. 1), but with a slightly smaller unit cell (378 versus 388 Å^3) attributed to the relatively stronger bonding between the Cu(II) and the pyrazine (Supplementary Data 1, Supplementary Table 2). The smaller unit cell of the Cu analogue is in good agreement with the relatively sharp pore size distribution analysis centred at 3.5 Å (average pore size), as determined from the CO_2 adsorption isotherms, using NLDFT model, which shows a smaller average pore size than the **SIFSIX**-3-Zn (3.5–4 Å) (Fig. 2a). The thermal gravimetric analysis of the **SIFSIX**-3-Cu showed a weight loss of about 10% for the dried sample in the range of 50–150 °C attributed to guest molecules (Supplementary Fig. 3). Further gradual loss was observed above 150 °C and attributed to the framework decomposition. The thermal gravimetric analysis data for the **SIFSIX**-3-Cu is in a good agreement with the one reported for the **SIFSIX**-3-Zn analogue. Infrared spectrum for the **SIFSIX**-3-Cu (Supplementary Fig. 4) exhibits bands characteristic of the C–H aromatic bonds associated to the pyrazine moiety at 3,114 and 3,073 cm^{-1} and bands characteristic for the C–N bond at 1,445, 1,122 and 1,070 cm^{-1}. Furthermore, the characteristic bands associated with the octahedral SiF_6 were also observed at 743 and 833 cm^{-1} (ref. 33).

CO_2 adsorption studies. In order to evaluate the potential of **SIFSIX**-3-Cu for CO_2 capture, we performed various CO_2 adsorption studies. It was our preconception that this new Cu analogue should at least show the same promising adsorption properties as the **SIFSIX**-3-Zn[23]. The Cu analogue shows even steeper variable temperature adsorption isotherms (Fig. 2a) at very low pressure indicative of relatively stronger CO_2- **SIFSIX**-3-Cu interactions than the Zn analogue

In order to further explore the possible sorption mechanistic behind this relatively enhanced uptake at low CO_2 loading, we explored the competitive adsorption kinetics of CO_2/N_2:10/90, CO_2/CH_4:50/50, CO_2/H_2:30/70 gas mixture adsorption (Supplementary Fig. 5). As anticipated and based on similar studies carried out on the Zn analogue[23], the uptake at equal times, including at equilibrium, for variable CO_2 compositions mixtures follows the behaviour of pure CO_2. These findings suggest that similarly to the mechanistic suggested for **SIFSIX**-3-Zn, when CO_2 containing mixtures are in contact with **SIFSIX**-3-Cu, CO_2 adsorbs more strongly (Supplementary Fig. 6) and rapidly than N_2 and by analogy also O_2, CH_4 and H_2 (Supplementary Fig. 5), thus occupying favourably most of the

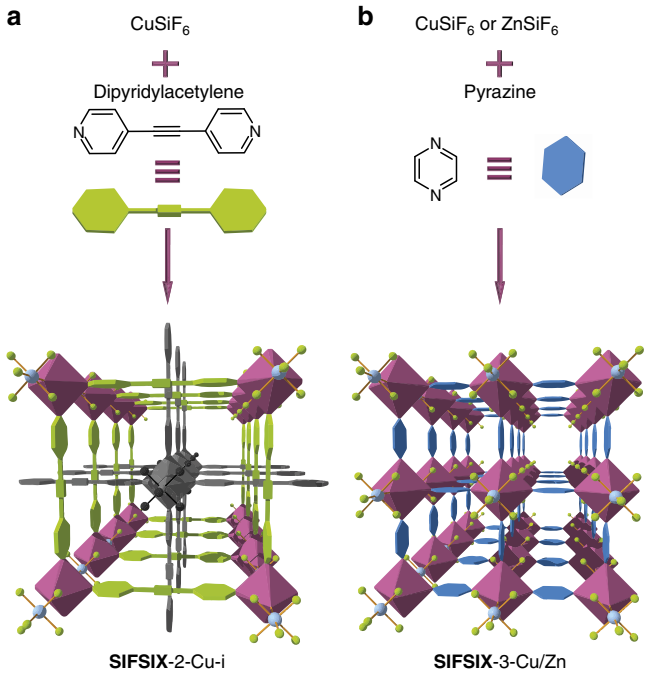

Figure 1 | Pore size tuning. Pore size tuning of the channel structures of (**a**) **SIFSIX**-2-Cu-i, (**b**) **SIFSIX**-3-Zn or/and **SIFSIX**-3-Cu. (**a**) **SIFSIX**-2-Cu-i; pores size 5.15 Å, Brunauer–Emmett–Teller (BET) apparent surface area (N_2 adsorption) 735 m^2 g^{-1}. (**b**) **SIFSIX**-3-Zn; pores size 3.84 Å, BET apparent surface area 250 m^2 g^{-1} (determined from the CO_2 adsorption isotherm at 298 K); **SIFSIX**-3-Cu; pores size 3.50 Å (NLDFT), BET and langmuir apparent surface area ca. 300 m^2 g^{-1} (determined from the CO_2 adsorption isotherm at 298 K). Colour code: Dipyridylacetylene (dpa, thick light green polygon), pyrazine (pyz, blue polygon), Zn, Cu (purple polyhedra), Si (light blue spheres), F (light green spheres). All guest molecules are omitted for clarity. Note that the grey net represents the interpenetrated net in **SIFSIX**-2-Cu-i.

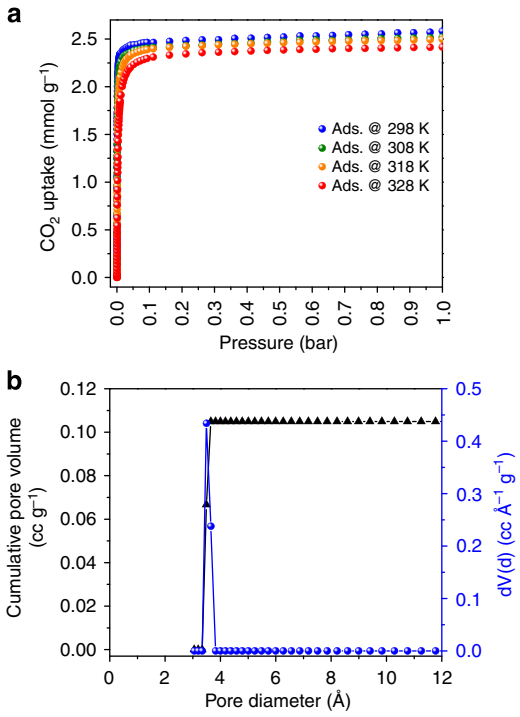

Figure 2 | CO_2 adsorption isotherms. CO_2 adsorption isotherms at variable temperatures for **SIFSIX**-3-Cu. The **SIFSIX**-3-Cu analogue shows asteeper variable temperature adsorption isotherms at very low pressure indicative of strong CO_2-**SIFSIX**-3-Cu interactions. (**a**) pore size distribution (PSD) derived from the CO_2 sorption isotherm (CO_2 at 273 K NLDFT) for **SIFSIX**-3-Cu. The PSD extracted from adsorption isotherms, shows an average pore size for **SIFSIX**-3-Cu centred at 3.5 Å(**b**).

© 2014 Macmillan Publishers Limited. All rights reserved.

available space and adsorption sites and subsequently exclude other gases, a desirable feature in many CO_2 separation and purification applications.

Interestingly, on the substitution of Zn by Cu, the Q_{st} of CO_2 adsorption in the contracted structure increased by 20%, from 45 to 54 kJ mol^{-1} (Fig. 3b), in perfect agreement with the relatively steeper CO_2 adsorption isotherms in the case of the Cu analogue at very low pressure.

Column breakthrough experiments. Furthermore, the CO_2 selectivity for **SIFSIX**-3-Zn and **SIFSIX**-3-Cu was investigated experimentally at trace CO_2 using column breakthrough tests for binary CO_2/N_2: 1,000 p.p.m./99.9% mixture (Fig. 4a) at 298 K in dry as well as in humid conditions. The derived selectivity at breakthrough time (and not equilibrium) is intended to reflect the real selectivity in real processes. In a dry condition, the first CO_2 signal downstream the column was observed only after ca. 798 and ca. 1,922 min g^{-1} for **SIFSIX**-3-Zn and **SIFSIX**-3-Cu, respectively, after starting continuous CO_2/N_2 gas mixture flux (5 cm^3 min^{-1}), while N_2 breakthrough occurred immediately in few seconds. Accordingly, at 1,000 p.p.m. CO_2 and breakthrough time, **SIFSIX**-3-Cu shows higher selectivity (ca. 10500) than **SIFSIX**-3-Zn (7259). It is to mention that calculated and measured selectivity exceeding 1,000–2,000 are often subject to uncertainties associated with measurement of the gas uptake of weakly adsorbed gases (N_2; Supplementary Fig. 6) in the mixture, thus the reported selectivity is aimed mainly for relative comparison of the studied compounds in this work. In view of that, a direct comparison between the **SIFSIX**-3-Cu and **the SIFSIX**-3-Zn sorption properties show a 50% relative increase in CO_2 selectivity at 1,000 ppm CO_2 in a N_2 stream (ca. 10500 versus 7259). The steeper CO_2 signal after breakthrough for **SIFSIX**-3-Cu as compared with the Zn analogue is a direct indication of the steeper CO_2 adsorption for the Cu analogue as shown in Fig. 3a.

Discussion

Recently, we reported CO_2 adsorption study on a series of isoreticular MOFs with periodically arrayed hexafluorosilicate (**SIFSIX**) pillars, called **SIFSIX**-2-Cu-i and **SIFSIX**-3-Zn (Fig. 1)[23]. The aforementioned porous MOFs having a combination of tunable pore size (rather than large surface area) coupled with the requisite chemistry led to materials with uniformly aligned strong CO_2 adsorption sites and subsequently

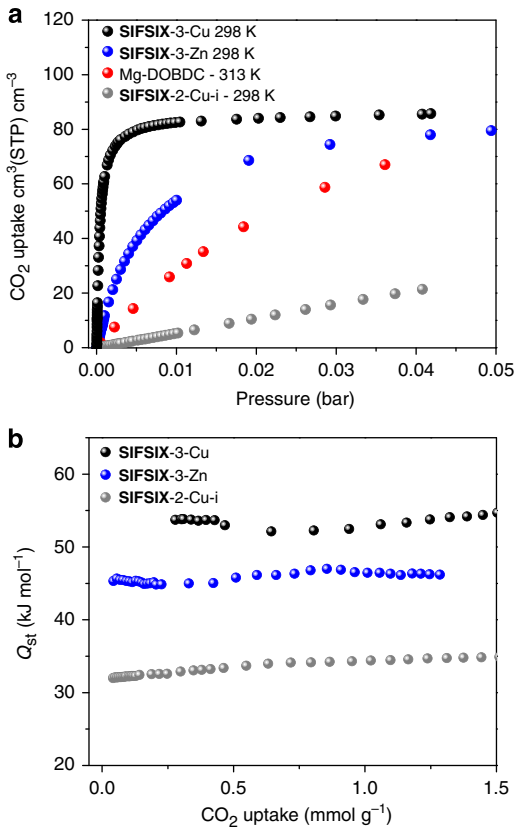

Figure 3 | CO_2 volumetric uptake. CO_2 volumetric uptake for **SIFSIX**-3-Cu at 298 K compared with **SIFSIX**-3-Zn, **SIFSIX**-2-Cu-I and Mg-MOF-74. The adsorption results at very low pressure (400 p.p.m.-5%) for the **SIFSIX**-3-Cu showed that the Cu analogue exhibits steeper adsorption isotherms at very low CO_2 concentration in comparison with other materials. At 7.6 torr (0.01 bar), **SIFSIX**-3-Cu uptakes 82.6 cm^3(STP)/cm^{-3} versus 55 and 28 cm^3(STP)/cm^{-3} for **SIFSIX**-3-Zn and Mg-MOF-74, respectively (**a**). Isosteric heats of adsorption at low coverage for **SIFSIX**-3-Cu, **SIFSIX**-3-Zn and **SIFSIX**-2-Cu-I. The Q_{st} for **SIFSIX**-3-Cu was observed to be higher than the Zn analogue and steady constant up to relatively higher recorded CO_2 loadings. This is indicative of the presence of homogenous binding sites over the full range of CO_2 loading for **SIFSIX**-3-Cu (**b**).

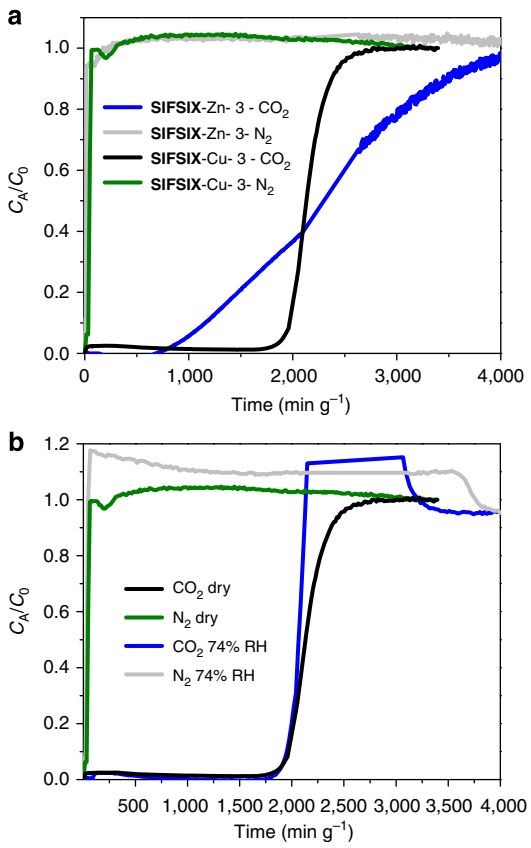

Figure 4 | Column breakthrough experiments. Column breakthrough test of CO_2/N_2:1,000 p.p.m./99.9% for **SIFSIX**-3-Cu, **SIFSIX**-3-Zn in dry condition (**a**). Column breakthrough test of CO_2/N_2:1,000 p.p.m./99.9% for **SIFSIX**-3-Cu in dry as well as at 74% RH (**b**). The CO_2 selectivity for **SIFSIX**-3-Zn and **SIFSIX**-3-Cu was investigated experimentally at trace CO_2 using column breakthrough tests for binary CO_2/N_2: 1,000 p.p.m./99.9% mixture at 298 K in dry as well as in humid conditions. In dry condition, the first CO_2 signal downstream the column was observed only after ca. 798 and ca. 1922 min g^{-1} for **SIFSIX**-3-Zn and **SIFSIX**-3-Cu, respectively, after starting continuous CO_2/N_2 gas mixture flux (5 cm^3 min^{-1}), while N_2 breakthrough occurred immediately in few seconds.

© 2014 Macmillan Publishers Limited. All rights reserved.

exhibiting a relatively fast and highly selective CO_2 behaviour over N_2, CH_4 and H_2 (ref. 23). Particularly, the denser isoreticular analogue, namely **SIFSIX**-3-Zn, revealed steeper variable CO_2 adsorption isotherms (Supplementary Fig. 7) than **SIFSIX**-2-Cu-i (Supplementary Fig. 8). This material exhibits unique key features suitable for post-combustion capture (that is, the CO_2 partial pressure of 100 mbar), as well as precombustion capture (that is, high CO_2 concentration and high pressure).

The pronounced steep CO_2 adsorption isotherms over a wide range of temperatures, particularly for this class of MOF materials, has inspired and compelled us to explore the potential of these **SIFSIX** MOFs for CO_2 adsorption in trace concentrations (that is, diluted streams in vacuum or in mixture containing a large fraction of N_2 up to 95%). In order to highlight the concealed potential of these MOFs for low CO_2 concentration applications (that is, involving CO_2 concentration below 5% or 50 mbar CO_2 partial pressure, such as anaesthesia machines and prepurification before air separation and air capture), single gas CO_2 adsorption properties were evaluated for **SIFSIX**-2-Cu-i and **SIFSIX**-3-Zn. Interestingly, the contraction of the pore size from 5.15 Å (for **SIFSIX**-2-Cu-i) to 3.84 Å (for **SIFSIX**-3-Zn) has prompted a drastic increase in CO_2 uptake (Supplementary Fig. 9) and consequently a recorded highest CO_2 uptake ever reported for a given MOF in the range under 5% CO_2. Specifically, **SIFSIX**-3-Zn showed an order of magnitude higher volumetric CO_2 uptake (55 cm^3 (STP)/cm^3) than to date best MOF materials such as Mg-MOF-74, (28 cm^3 (STP)/ cm^3) at 10 mbar (1% CO_2), while UTSA-16 (ref. 34), exhibits much lower CO_2 uptake similar to **SIFSIX**-2-Cu-i.

The noticeable impact of pore size contraction on the adsorption energetics and uptake has impelled us to explore various pathways to further reduce the pore size of the **SIFSIX**-3-M derivative via metal substitution and evaluate its effect on the CO_2 adsorption properties. The rational is based on conventional coordination chemistry suggesting that replacement of Zn(II) by Cu(II) to form an isostructural **SIFSIX**-3-Cu will potentially induce an additional pore contraction due to Jahn–Teller distortions of the octahedral coordination geometry of Cu(II), CuN_4F_2. The Cu(II) has an open shell valence electron configuration $3d^9$, in contrast to Zn(II) with a close shell $3d^{10}$, and thus will experience a distorted octahedral coordination geometry with potentially elongated Cu–F (fluorine) bonds and relatively shorter Cu–N (nitrogen) bonds (Supplementary Fig. 10 and Supplementary Table 2). Indeed, our analysis of readily available coordination polymers constructed from hexafluorosilicate ions with pyrazine supports our proposal and shows that the bonding of the Cu(II) with pyrazine leads to a slightly shorter M–N bond than the zinc analogue (see Supplementary Table 2)[35]. Accordingly, it is anticipated that successful substitution of Zn(II) by Cu(II) will permit access to the desired isostructural **SIFSIX**-3-Cu with relatively contracted pore size than the parent **SIFSIX**-3-Zn analogue and subsequent evaluation of its relative CO_2 adsorption properties.

Examination of the **SIFSIX**-3-M adsorption results in the spectra of low-concentration applications (400 p.p.m.-5%) showed that the Cu analogue exhibits even steeper adsorption isotherms at very low CO_2 concentration (Fig. 3a) translated into the highest uptake ever reported for MOFs without unsaturated metal centres or exposed amino functionality at low CO_2 pressures below 38 torr (0.05 bar). This unprecedented finding is even more appealing owing to its fully physical adsorption nature where complete desorption of CO_2 was established under vacuum at only 323 K. At 7.6 torr (0.01 bar) **SIFSIX**-3-Cu uptakes 82.6 cm^3(STP).cm^{-3} versus 55 and 28 cm^3(STP).cm^{-3} for **SIFSIX**-3-Zn and Mg-MOF-74, respectively. Interestingly, the gravimetric uptake of **SIFSIX**-3-Cu at 400 p.p.m. and 298 K (1.24 mmol g^{-1}) is ca. 10 and 15 times higher than the corresponding uptakes for **SIFSIX**-3-Zn (0.13 mmol g^{-1}) and Mg-MOF-74 (0.08 mmol g^{-1}) and even higher than the observed uptakes for most amine-supported silica materials (with optimal compromise of amine loading and kinetics)[22] at 298 K (for example TRI-PE-MCM-4 (1 mmol g^{-1})[10,22]). Table 1 summarizes the CO_2 adsorption uptake at variable low CO_2 concentration (partial pressures) for **SIFSIX** compounds as compared with Mg-MOF-74 and amine-supported materials (including MOFs), relevant to different trace CO_2 removal applications. It is to notice that **SIFSIX**-3-Cu shows even higher CO_2 uptake at 400 p.p.m. and 328 K as compared with the corresponding uptake at 323 K for amine functionalized Mg-dobpdc-mmen (Supplementary Table 3).

This increase is mainly attributed to the contracted pore size of the Cu analogue, which in turn (i) results in a relative increase of the charge density surrounding the adsorbed CO_2 molecules and (ii) favors the relatively faster CO_2 adsorption kinetics in comparison with N_2. Indeed, the four flourine atoms pointing to the channel, in the same plane, are creating a proximal local charge density to the adsorbed CO_2 molecule, that is, the CO_2–F average distance is much narrower in the case of the Cu analogue

Table 1 | CO_2 adsorption uptake comparison.

Adsorbent	Uptake at 400 p.p.m. (0.4 mbar)	Uptake at 5,000 p.p.m. (5 mbar)	Uptake at 10,000 p.p.m. (10 mbar)	CO_2 Qst (kJ mol^{-1})
SIFSIX-2-Cu-i	0.0684*/0.2†	0.097*/2.7†	0.19*/5.32†	32
SIFSIX-3-Zn	0.13*/5.6†	1.12*/39.26†	1.53*/53.97†	45
SIFSIX-3-Cu	**1.24*/43.9†**	**2.26*/79.8†**	**2.34*/82.5†**	**54**
Mg-MOF-74	0.088*/1.8†	0.7*/14.3†	1.27*/25.86†	47
Mg-MOF-74-ED§,‖	1.5*	ND	ND	ND
Mg-dobpdc-mmen‖,¶	2*	2.5*	2.75*	70
TRI-PE-MCM-41‖,#	1*	1.45*	1.6*	92
HAS‖#	1.7*	ND	ND	ND

ND, non determined.
CO_2 adsorption uptake at various traces of CO_2 concentration and at 298 K in comparison with the most promising MOFs and other various amine-supported materials.
*mmol g^{-1}.
†cm^3 (STP)/cm^3.
§Ethylenediamine functionalized[28].
‖Chemical adsorbent.
¶*N, N*-dimethylethylenediamine functionalized[27].
#Amine-supported silica.
Data in bold represents the data reported for the MOF reported in this work.

© 2014 Macmillan Publishers Limited. All rights reserved.

than the relatively open Zn analogue. It is suggested that the relatively narrower pore size allows and reinforces each CO_2 molecule to interact mutually with four fluorine centres, that is, the CO_2 molecule can interact potentially with four different surfaces of the square encompassing four fluorine adsorption sites at the same time. The Q_{st} of CO_2 adsorption is an intrinsic property that dictates the affinity of the pore surface toward CO_2; this in turn plays a major role in determining the adsorption selectivity and the necessary energy to release CO_2 during the regeneration step. Although the Q_{st} for CO_2 was slightly above the typical range of fully reversible CO_2 adsorption (30–50 kJ mol^{-1})[22], **SIFSIX**-3-Cu was fully and promptly evacuated at 323 K in vacuum (or under N_2 flow environment). As in case of **SIFSIX**-3-Zn and **SIFSIX**-2-Cu-i, the Q_{st} for CO_2 adsorption was steady constant up to relatively high CO_2 loadings indicating homogenous binding sites over the full range of CO_2 loading (Fig. 3b))[23]. The aforementioned competitive sorption kinetics of CO_2/N_2:10/90, CO_2/CH_4:50/50, CO_2/H_2:30/70 gas mixture adsorption experiments (Supplementary Fig. 3) suggest a relatively high selective CO_2 adsorption that is plausible due to a synergistic interplay between CO_2 sorption thermodynamics and kinetics. This high selectivity was confirmed by performing prediction of CO_2/N_2 gas mixture adsorption at equilibrium using Ideal Adsorption Solution Theory (Supplementary Fig. 11). It is important to notice that the derived selectivity at breakthrough time is non-equilibrium data where, similarly to equilibrium Ideal Adsorption Solution Theory results, a complex interplay between strong electrostatic interactions and favourable kinetics toward CO_2 drive the high selectivity of CO_2 versus N_2. The experimental results of the CO_2/N_2 gas mixture adsorption testing in dry and humid conditions revealed that the CO_2 apparent selectivity at 1,000 p.p.m. CO_2 on **SIFSIX**-3-Cu was not affected by the presence of humidity as shown from the column breakthrough tests performed on both compounds at the relative humidity (RH) of 74% (Fig. 4a). This unprecedented finding was also valid in case of **SIFSIX**-3-Zn for the removal of low and higher CO_2 concentration[23].

Finally, as was demonstrated for **SIFSIX**-3-Zn, **SIFSIX**-3-Cu is a recyclable and moisture stable MOFs as inferred from the PXRD performed on associated samples after at least four cycles of CO_2 adsorption and breakthrough runs under dry and humid conditions (74% RH) (Supplementary Fig. 12).

In conclusion, we showed herein how a material design and engineering approach to pore size control in combination with suitable energetics of favourable electrostatics from an array of inorganic anions affords novel **SIFSIX**-3-Cu MOF with exceptional CO_2 uptake and selectivity in the context of air capture and trace CO_2 removal. This unique material exhibits very high CO_2 sorption energetics but fully reversible physical driven adsorption–desorption operations at very mild conditions, without the well-documented drawbacks associated with amine reactive chemistry.

This work shows for the first time that MOFs, thanks to their ability for rational pore size modification and inorganic-organics moieties substitution, offer remarkable CO_2 physical adsorption attributes in highly diluted gas streams that other class of plain materials are unable to attain. Further work is underway to use the learning gained in the case of **SIFSIX**-3-M compounds to develop topologically and chemically different MOFs, aiming to target novel MOFs with suitable pore size and high charge density, for use in trace CO_2, low and high concentration CO_2 removal.

Methods

Preparation of SIFSIX-3-Cu. A methanol solution (5.0 ml) of pyrazine (pyz, 0.30 g, 3.0 mmol) was layered in a glass tube onto a methanol solution (5.0 ml) of $CuSiF_6 \times H_2O$ (0.325 g, 0.6 mmol). On layering, a fast formation of light violet powder was observed, and the powder was left for 24 h in the mother solution. The powder was then collected and washed extensively with methanol and then dried under vacuum.

Characterization. The PXRD patterns were recorded using a Panalytical X'pert PRO MPD X-ray Diffractometer with Cu Kα radiation ($\lambda = 0.15418$ nm, 45 kV, 40 mA).

Low-pressure adsorption. The low-pressure gas sorption isotherms were collected on Autosorb-1C (Quantachrome Instruments) Surface Area and Porosity Analyzer after activation of **SIFSIX-3-Cu** as follows. As-synthesized **SIFSIX-3-Cu** was exchanged with methanol for 3 days. The sample was degassed at room temperature under high vacuum (<5 μm Hg) for 12 h, then to 323 K for another 12 h before adsorption analysis. The apparent surface areas of **SIFSIX-3-Cu** were determined from the CO_2 adsorption isotherm collected at 298 K, respectively by applying the BET and Langmuir models. The determination of the isosteric heat of adsorption (Q_{st}) for CO_2 was estimated by applying the Clausius–Clapeyron expression using the CO_2 adsorption isotherms measured at 298, 308, 318 and 328 K. The bath temperature was precisely controlled using a Julabo recirculating control system containing a mixture of ethylene glycol and water. Data points below 0.76 Torr were not used for this calculation, in order to avoid possible artifacts at very low coverage.

Measurement of equilibrium and kinetics of adsorption. Adsorption equilibrium measurements of pure gases were performed using a Rubotherm gravimetric–densimetric apparatus (Bochum, Germany) (Supplementary Fig. 13), composed mainly of a magnetic suspension balance and a network of valves, mass flowmeters and temperature and pressure sensors. The magnetic suspension balance overcomes the disadvantages of other commercially available gravimetric instruments by separating the sensitive microbalance from the sample and the measuring atmosphere and is able to perform adsorption measurements across a wide pressure range, that is, from 0 to 20 MPa. The adsorption temperature may also be controlled within the range of 77 to 423 K. In a typical adsorption experiment, the adsorbent is precisely weighed and placed in a basket suspended by a permanent magnet through an electromagnet. The cell in which the basket is housed is then closed and vacuum or high pressure is applied. The gravimetric method allows the direct measurement of the reduced gas adsorbed amount Ω. Correction for the buoyancy effect is required to determine the excess and absolute adsorbed amount using equations 1 and 2, where $V_{adsorbent}$ and V_{ss} and $V_{adsorbed}$ phase refer to the volume of the adsorbent, the volume of the suspension system and the volume of the adsorbed phase, respectively.

$$\Omega = m_{absolute} - \rho_{gas}\left(V_{adsorbent} + V_{ss} + V_{adsorbed\text{-}phase}\right) \quad (1)$$

$$\Omega = m_{excess} - \rho_{gas}\left(V_{adsorbent} + V_{SS}\right) \quad (2)$$

The buoyancy effect resulted from the adsorbed phase maybe taken into account via correlation with the pore volume or with the theoretical density of the sample.

Kinetic studies of CO_2 and CO_2/N_2:10/90 adsorption on **SIFSIX**-3-Cu was carried out using the Rubotherm gravimetric apparatus operating in dynamic regime. Initially, **SIFSIX**-3-Cu was properly evacuated at 323 K in vacuum. In order to achieve an immediate constancy of pressure (0.5 bar) during kinetics tests and avoid the often noisy uptake during the rapid introduction of the studied gas, an initial baseline was set-up using helium gas at 0.5 bar for single gases and 1 bar for mixture, then the studied single gas or mixture is flushed with a flow of 300 ml min^{-1} to avoid any dependence of the kinetics on the mass flow controller.

Column breakthrough tests. The experimental set-up used for dynamic breakthrough measurements is shown in Supplementary Fig. 13. The gas manifold consisted of three lines fitted with mass flow controllers Line 'A' is used to feed an inert gas, most commonly helium, to activate the sample before each experiment. The other two lines, 'B' and 'C' feed a mixture of CO_2 and other gases like N_2, CH_4 and H_2. Hence, gas mixtures with concentrations representative of different industrial gases may be prepared. Whenever required, gases flowing through lines 'B' and 'C' may be mixed before entering a column packed with **SIFSIX**-3-Cu using a four-way valve. The stainless steel column was 27 mm in length with 4 mm of inner (6.4 mm outer) diameter. The column downstream was monitored using a Hiden analytical mass spectrometer. In a typical experiment, 0.1–0.4 g of adsorbent was treated at 298 K overnight under helium flow of 5 ml min^{-1} at 323 K, then the gas flow was switched to the desired gas mixture at the same flow rate. The complete breakthrough of CO_2 and other species was indicated by the downstream gas composition reaching that of the feed gas. Experiments in the presence of 74% RH were performed by flowing the gas mixture through water vapour saturator at 20 °C.

The selectivity of CO_2 over N_2 is calculated using the equation below:

$$S_{\frac{CO_2}{N_2}} = \frac{(\text{Uptake } CO_2/\text{Uptake } CO_2 \text{ and } N_2)/(\text{Uptake } N_2/\text{Uptake } CO_2 \text{ and } N_2)}{\text{Composition } CO_2/\text{Composition } N_2} \quad (3)$$

© 2014 Macmillan Publishers Limited. All rights reserved.

References

1. Lackner, K. S. & Wright, A. B. Removal of carbon dioxide from air. WO 2010022399 A1 (2010).
2. Major, C. J., Sollami, B. J. & Kammerme, K. Carbon dioxide removal from air by adsorbents.. *Ind. Eng. Chem. Process Des. Dev.* **4,** 327–333 (1965).
3. Stolaroff, J. K., Keith, D. W. & Lowry, G. V. Carbon dioxide capture from atmospheric air using sodium hydroxide spray. *Environ. Sci. Technol.* **42,** 2728–2735 (2008).
4. Nikulshina, V., Gebald, C. & Steinfeld, A. CO_2 capture from atmospheric air via consecutive CaO-carbonation and $CaCO_3$-calcination cycles in a fluidized-bed solar reactor. *Chem. Eng. J.* **146,** 244–248 (2009).
5. Goeppert, A., Czaun, M., Prakash, G. K. S. & Olah, G. A. Air as the renewable carbon source of the future: An overview of CO_2 capture from the atmosphere. *Energ. Environ. Sci.* **5,** 7833–7853 (2012).
6. Rege, S. U., Yang, R. T. & Buzanowski, M. A. Sorbents for air prepurification in air separation. *Chem. Eng. Sci.* **55,** 4827–4838 (2000).
7. Rege, S. U., Yang, R. T., Qian, K. Y. & Buzanowski, M. A. Air-prepurification by pressure swing adsorption using single/layered beds. *Chem. Eng. Sci.* **56,** 2745–2759 (2001).
8. Santos, J. C., Magalhaes, F. D. & Mendes, A. Contamination of zeolites used in oxygen production by PSA: effects of water and carbon dioxide. *Ind. Eng. Chem. Res.* **47,** 6197–6203 (2008).
9. Haring, H. W. *Industrial Gases Processing* (Wiley-VCH Verlag GmbH & Co, 2008).
10. Belmabkhout, Y., Serna-Guerrero, R. & Sayari, A. Amine-bearing mesoporous silica for CO_2 removal from dry and humid air. *Chem. Eng. Sci.* **65,** 3695–3698 (2010).
11. Kordesch, K. *et al.* Alkaline fuel cells applications. *J. Power Sources* **86,** 162–165 (2000).
12. Ernsting, J. Breathing systems in aerospace. IEE Seminar. Low Flow Anaesthesia Breathing Systems-Technology, Safety and Economics (Ref. No.1999/060), 7/1-4 (1999).
13. Satyapal, S., Filburn, T., Trela, J. & Strange, J. Performance and properties of a solid amine sorbent for carbon dioxide removal in space life support applications. *Energ. Fuel* **15,** 250–255 (2001).
14. Mattox, E. M., Knox, J. C. & Bardot, D. M. Carbon dioxide removal system for closed loop atmosphere revitalization, candidate sorbents screening and test results. *Acta Astronaut.* **86,** 3946 (2013).
15. Moore, P. Miner protection. *Min. Mag.* **196,** 35–41 (2007).
16. Dosch, M. P. The anesthesia gas machine http://www.udmercy.edu/crna/agm (2006).
17. Dosch, M. P. The anesthesia gas machine http://www.udmercy.edu/crna/agm/07.htm (2012).
18. Wilmer, C. E., Farha, O. K., Bae, Y.-S., Hupp, J. T. & Snurr, R. Q. Structure-property relationships of porous materials for carbon dioxide separation and capture. *Energ. Environ. Sci.* **5,** 9849–9856 (2012).
19. Sayari, A. & Belmabkhout, Y. Stabilization of amine-containing CO_2 adsorbents: dramatic effect of water vapor. *J. Am. Chem. Soc.* **132,** 6312–6313 (2010).
20. Caskey, S. R., Wong-Foy, A. G. & Matzger, A. J. Dramatic tuning of carbon dioxide uptake via metal substitution in a coordination polymer with cylindrical pores. *J. Am. Chem. Soc.* **130,** 10870–10871 (2008).
21. Sumida, K. *et al.* Carbon dioxide capture in metal-organic frameworks. *Chem. Rev.* **112,** 724–781 (2012).
22. Sayari, A., Belmabkhout, Y. & Serna-Guerrero, R. Flue gas treatment via CO_2 adsorption. *Chem. Eng. J.* **171,** 760–774 (2011).
23. Nugent, P. *et al.* Porous materials with optimal adsorption thermodynamics and kinetics for CO_2 separation. *Nature* **495,** 80–84 (2013).
24. Xue, D. X. *et al.* Tunable rare-earth fcu-MOFs: A platform for systematic enhancement of CO_2 adsorption energetics and uptake. *J. Am. Chem. Soc.* **135,** 7660–7667 (2013).
25. Choi, S., Drese, J. H., Eisenberger, P. M. & Jones, C. W. Application of amine-tethered solid sorbents for direct CO_2 capture from the ambient air. *Environ. Sci. Technol.* **45,** 2420–2427 (2011).
26. Goeppert, A., Czaun, M., Surya Prakash, G. K. & Olah, G. A. Air as the renewable carbon source of the future: an overview of CO_2 capture from the atmosphere. *Energy Environ. Sci.* **5,** 7833–7853 (2012).
27. McDonald, T. M. *et al.* Capture of carbon dioxide from air and flue gas in the alkylamine-appended metal-organic framework mmen-Mg_2(dobpdc). *J. Am. Chem. Soc.* **134,** 7056–7065 (2012).
28. Choi, S., Watanabe, T., Bae, T.-H., Sholl, D. S. & Jones, C. W. Modification of the Mg-DOBDC MOF with amines to enhance CO_2 adsorption from ultradilute Gases. *J. Phys. Chem. Lett.* **3,** 1136–1141 (2012).
29. Guillerm, V. *et al.* Porous organic polymers with anchored aldehydes: A new platform forpost-synthetic amine functionalization en route for enhanced CO_2 adsorption properties. *Chem. Commun.* **50,** 1937–1940 (2013).
30. Le Bail, A. Monte Carlo indexing with McMaille. *Powder Diffr.* **19,** 249–254 (2004).
31. Le Bail, A., Duroy, H. & Fourquet, J. L. *Ab-initio* structure determination of $LiSbWO_6$ by X-ray powder diffraction. *Mater. Res. Bull.* **23,** 447–452 (1988).
32. Rodriguez-Carvajal, J. Abstracts of the Satellite. *Meeting on Powder Diffraction of the XV Congress of the IUCr*, 127 (1990).
33. Conley, B. D., Yearwood, B. C., Parkin, S. & Atwood, D. A. Ammonium hexafluorosilicate salts. *J. Fluorine Chem.* **115,** 155–160 (2002).
34. Xiang, S. *et al.* Microporous metal-organic framework with potential for carbon dioxide capture at ambient conditions. *Nat. Commun.* **3,** 956–965 (2012).
35. Uemura, K., Maeda, A., Maji, T. K., Kanoo, P. & Kita, H. Crystal structures and adsorption properties of ultramicroporous coordination polymers constructed ions from hexafluorosilicate ions and pyrazine. *Eur. J. Inorg. Chem.* 2329–2337 (2009).

Acknowledgements

Research reported in this publication was supported by the King Abdullah University of Science and Technology (KAUST).

Author contributions

O.S., Y.B. and M.E. contributed to the conceptual approach in designing the synthetic experiments; O.S. and Z.C. carried out the synthetic experiments; V.G. and K.A. conducted and interpreted the crystallographic experiments; Y.B. and A.C. conducted and interpreted low-pressure sorption experiments; Y.B. conducted and interpreted column breakthrough experiments; O.S., Y.B. and M.E. wrote the manuscript.

Additional information

Accession codes: The X-ray crystallographic data for structure reported in this article has been deposited at the Cambridge Crystallographic Data Centre (CCDC), under deposition number CCDC 970790. The data can be obtained free of charge from The Cambridge Crystallographic Data Center via www.ccdc.cam.ac.uk/data_request/cif.

Supplementary Information accompanies this paper at http://www.nature.com/naturecommunications

Competing financial interests: The authors declare no competing financial interests.

Reprints and permission information is available online at http://npg.nature.com/reprintsandpermissions/

How to cite this article: Shekhah, O. *et al.* Made-to-order metal-organic frameworks for trace carbon dioxide removal and air capture. *Nat. Commun.* 5:4228 doi: 10.1038/ncomms5228 (2014).

This work is licensed under a Creative Commons Attribution-NonCommercial-NoDerivs 4.0 International License. The images or other third party material in this article are included in the article's Creative Commons license, unless indicated otherwise in the credit line; if the material is not included under the Creative Commons license, users will need to obtain permission from the license holder to reproduce the material. To view a copy of this license, visit http://creativecommons.org/licenses/by-nc-nd/4.0/

© 2014 Macmillan Publishers Limited. All rights reserved.